

Enhanced stability of FA-based perovskite: Rare-earth metal compound $EuBr_2$ doping

Minna Hou(侯敏娜), Xu Guo(郭旭), Meidouxue Han(韩梅斗雪), Juntao Zhao(赵均陶), Zhiyuan Wang(王志元), Yi Ding(丁毅), Guofu Hou(侯国付), Zongsheng Zhang(张宗胜), and Xiaoping Han(韩小平)

Citation: Chin. Phys. B, 2024, 33 (**4**): 047802. DOI: 10.1088/1674-1056/ad23d5
Journal homepage: http://cpb.iphy.ac.cn; http://iopscience.iop.org/cpb

What follows is a list of articles you may be interested in

Shape and diffusion instabilities of two non-spherical gas bubbles under ultrasonic conditions

Wurihan Bao(包乌日汗) and De-Xin Wang(王德鑫)
Chin. Phys. B, 2024, 33 (**1**): 017803. DOI: 10.1088/1674-1056/acfa81

Improving efficiency of inverted perovskite solar cells via ethanolamine-doped PEDOT:PSS as hole transport layer

Zi-Jun Wang(王子君), Jia-Wen Li(李嘉文), Da-Yong Zhang(张大勇), Gen-Jie Yang(杨根杰), and Jun-Sheng Yu(于军胜)
Chin. Phys. B, 2022, 31 (**8**): 087802. DOI: 10.1088/1674-1056/ac5988

First principles investigation on Li or Sn codoped hexagonal tungsten bronzes as the near-infrared shielding material

Bo-Shen Zhou(周博深), Hao-Ran Gao(高浩然), Yu-Chen Liu(刘雨辰), Zi-Mu Li(李子木),Yang-Yang Huang(黄阳阳), Fu-Chun Liu(刘福春), and Xiao-Chun Wang(王晓春)
Chin. Phys. B, 2022, 31 (**5**): 057804. DOI: 10.1088/1674-1056/ac598a

A flexible ultra-broadband metamaterial absorber working on whole K-bands with polarization-insensitive and wide-angle stability

Tao Wang(汪涛), He-He He(何贺贺), Meng-Di Ding(丁梦迪), Jian-Bo Mao(毛剑波), Ren Sun(孙韧), and Lei Sheng(盛磊)
Chin. Phys. B, 2022, 31 (**3**): 037804. DOI: 10.1088/1674-1056/ac306e

Enhancing the photo-luminescence stability of $CH_3NH_3PbI_3$ film with ionic liquids

Weifeng Ma(马威峰), Chunjie Ding(丁春杰), Nasrullah Wazir, Xianshuang Wang(王宪双), Denan Kong(孔德男), An Li(李安), Bingsuo Zou(邹炳锁), and Ruibin Liu(刘瑞斌)
Chin. Phys. B, 2022, 31 (**3**): 037802. DOI: 10.1088/1674-1056/ac3067

Enhanced stability of FA-based perovskite: Rare-earth metal compound $EuBr_2$ doping

Minna Hou(侯敏娜)[1], Xu Guo(郭旭)[1], Meidouxue Han(韩梅斗雪)[2], Juntao Zhao(赵均陶)[2], Zhiyuan Wang(王志元)[1], Yi Ding(丁毅)[2,†], Guofu Hou(侯国付)[2], Zongsheng Zhang(张宗胜)[1], and Xiaoping Han(韩小平)[1,‡]

[1] *School of Energy and Power Engineering, North University of China, Taiyuan* 030051, *China*
[2] *Institute of Photoelectronic Thin Film Devices and Technology, Nankai University, Tianjin* 300072, *China*

(Received 15 November 2023; revised manuscript received 16 January 2024; accepted manuscript online 30 January 2024)

It is highly desirable to enhance the long-term stability of perovskite solar cells (PSCs) so that this class of photovoltaic cells can be effectively used for the commercialization purposes. In this contribution, attempts have been made to use the two-step sequential method to dope $EuBr_2$ into $FAMAPbI_3$ perovskite to promote the stability. It is shown that the device durability at 85 °C in air with RH of 20%–40% is improved substantially, and simultaneously the champion device efficiency of 23.04% is achieved. The enhancement in stability is attributed to two points: (i) $EuBr_2$ doping effectively inhibits the decomposition and α–δ phase transition of perovskite under ambient environment, and (ii) $EuBr_2$ aggregates in the oxidized format of $Eu(BrO_3)_3$ at perovskite grain boundaries and surface, hampering humidity erosion and mitigates degradation through coordination with H_2O.

Keywords: $EuBr_2$ doping, inhibited phase transition and decomposition, stability, perovskite solar cell

PACS: 88.40.H–, 88.40.hj **DOI:** 10.1088/1674-1056/ad23d5

1. Introduction

Perovskite solar cells (PSCs) have experienced rapid development during the past decades, and the certified efficiency of 26.1% has been achieved.[1] With respect to the efficiency, the stability of PSCs is not so easy to be improved significantly. Although many attempts have been done through various strategies like encapsulation and interface engineering,[2–6] the enhancement in stability still cannot meet the requirement of commercialization.[7,8] Fundamentally, it is due to the intrinsic properties of perovskite absorber: (i) highly efficient perovskite absorber $FAPbI_3$ spontaneously transforms from α phase to δ phase at room temperatures,[9,10] and (ii) the structure decomposition would easily occur under external aging factors due to the weak binding between organic cation and inorganic framework.[11–15] Undoubtedly, the undesired intrinsic stability of perovskite greatly limits the wide applications of PSCs.

To solve two fundamental problems stated above, two methods are often used: the first is to tailor the bulk perovskite into the two-dimensional (2D) structure based on the hydrophobicity and Van der Waals interaction of bulkier organic cation,[16,17] and the second is to incorporate dopants into the perovskite system.[18–23] Recently, the latter provokes great research interest. For example, You *et al.* reported that rubidium (Rb) doping stabilized perovskite by forming secondary-phase $(PbI_2)_2RbCl$.[24] Another dopant europium (Eu) was also observed to improve the stability of perovskite by several groups.[25,26] Xiang *et al.*'s study showed that EuI_2 doping into inorganic $CsPbI_2Br$ remarkably enhances the thermodynamic stability,[27] which can be attributed to two points: (i) Eu occupies the B site of perovskite to increase the tolerance factor and lower the lattice distortion, and (ii) the Eu doping increases the surface-to-volume ratio to enhance the surface energy. Wang *et al.* studied the effect of $Eu(acac)_3$ doping on organic–inorganic hybrid perovskite, and found that the operating stability is enhanced through using Eu^{3+}–Eu^{2+} as redox shuttle to selectively oxidize Pb^0 and reduce I^0 in the cyclical transition. Moreover, the thermodynamic stability of $MAPbI_3$ system was investigated by intercalating Eu between crystal lattices.[28] However, there is a notable lack of investigations of the effect of Eu doping on phase and structure stability of $FAPbI_3$, which is desired for further progress toward FA-based perovskite solar cells.

Herein, we systematically explore the effect of $EuBr_2$ doping on the phase and structure stability of $FAPbI_3$ thin film and solar cell, and the associated mechanisms as well. It is revealed that the appropriate amount of $EuBr_2$ doping hardly influences the crystallinity and optoelectronic properties of $FAPbI_3$ thin film, but effectively inhibits the phase transition and decomposition of $FAPbI_3$. The XPS measurement shows that Eu^{3+} and BrO^{3-} form at the grain boundaries and surface of perovskite, hindering the environmental erosion and mitigating the degradation process of perovskite. Consequently, $EuBr_2$doping causes the device stability to be remarkably improved.

†Corresponding author. E-mail: yiding@nankai.edu.cn
‡Corresponding author. E-mail: xiaopinghan@nuc.edu.cn

© 2024 Chinese Physical Society and IOP Publishing Ltd

2. Experiment method

2.1. Materials

All the chemicals and solvents were purchased from commercial sources and used as received without further purification unless stated otherwise. SnO_2 colloid liquid was purchased from Alfa Aesar. $EuBr_2$ was purchased from TCI. Bis(trifluoromethane) sulfonimide lithium salt (Li-TFSI), 4-tert-butylpyridine (tBP), chlorobenzene, dimethylsulfoxide (DMSO), N,N-dimethylformamide (DMF), and isopropyl alcohol (IPA) were purchased from Sigma-Aldrich. Formamidinium iodide (FAI), methylammonium iodide (MAI), and methylammonium chloride (MACl), Spiro-OMeTAD were purchased from Xi'an Polymer Light Technology Corp.

2.2. Device fabrication

Planar n–i–p solar cells with conventional structure of ITO/ SnO_2/perovskite/Spiro-OMeTAD/Au were fabricated by two-step method in the N_2 glove box. The ITO substrates with a sheet resistance of 10 Ω/sq were washed with detergent, deionized water, and IPA sequentially. The cleaned ITO substrates were treated by ultraviolet (UV)-ozone for 20 min before subsequent spin-coating. Then the diluted SnO_2 liquid was spin-coated on the pre-cleaned substrate at 4000 r for 30 s and annealed at 150 °C for 30 min. The SnO_2 substrate was treated by UV-ozone for 20 min, and then transferred to glove box to continue subsequent deposition. $EuBr_2$ solution was prepared by dissolving 10-mg $EuBr_2$ in 1-mL mixed solvent of DMF and DMSO. 1.5-M PbI_2 precursor was prepared by dissolving PbI_2 in mixed solvent of DMF and DMSO. Organic salt precursor solution was composed of 90-mg FAI, 6.39-mg MAI, 9-mg MACl, and 1-mL IPA. PbI_2 and FAI/MAI/MACl precursor solution was prepared and stirred over night before use. 50-μL PbI_2 solution was spin-coated onto SnO_2 layer at 1500 r for 30 s. The resultant film was annealed at 70 °C. After the PbI_2 film cooled to room temperature, 50-μL FAI/MAI/MACl solution was dropped on the PbI_2 film quickly and spun at 2000 r immediately for 30 s. Subsequently, the sample was annealed at 150 °C for 20 min to form perovskite layer. 35-μL Spiro-OMeTAD solution, which was prepared by dissolving 72.3-mg Spiro-OMeTAD, 30-μL tBP, and 35-μL LiTFSI stock solution (260-mg LiTFSI in 1-mL acetonitrile) in 1-mL chlorobenzene, was spin-coated at 3000 r to form HTL. Finally, gold was evaporated as electrode.

2.3. Characterization

The *J*–*V* curves were measured in N_2 glove box under AM 1.5G illumination with a Keithley2400 digital source meter calibrated by Asahi Spectra Co., Ltd. During current–voltage measurements for all samples. A metal mask of 0.089 cm^2 was used to reduce the influence of the scattered light during the measurement. SEM images were recorded using field emission scanning electron microscope (Jeol JSM-6700F, Japan). UV-Vis spectra were measured through a UV-Vis-NIR spectrophotometer Cary 5000, Varian, USA. PL spectra and TRPL spectra were recorded through Fluorolog–Horiba fluorometer (FLS980, Edinburgh Instruments, UK) with excitation wavelength of 470 nm. XPS measurements were performed with a PHI VersaProbe II scanning XPS microprobe with a spot size of 500 μm. XRD spectra were recorded on Mini Flex 600, Rigaku, Japan in the 2θ range from 1° to 60°. FTIR spectra were measured by Therm Nicolet iS10 instrument.

3. Results and discussion

Two-step sequential spin-coating technique was employed to fabricate perovskite films, and $EuBr_2$ was added into PbI_2 precursor solution to achieve effective doping. Comparing the SEM images of control and $EuBr_2$-doped perovskite films (Figs. 1(a) and 1(b)), one can see that $EuBr_2$ doping causes the crystallinity of perovskite film to deteriorate slightly. The similar phenomenon can be observed in the x-ray diffraction (XRD) measurement on the control and $EuBr_2$-doped perovskite films (see Fig. 1(c)), where the diffractions of both PbI_2 and the perovskite (110) show a little reduction in intensity. The slightly deteriorated crystallinity of perovskite film may be caused by the $EuBr_2$ distributed at grain boundary which we will discuss later.

The optoelectronic property of perovskite films was also studied by photoluminescence (PL) spectra and time-resolved photoluminescence (TRPL) measurements. It is clear from Fig. 1(d) that the incorporation of europium gives rise to a slight blue-shift in PL spectra, thus inducing a slight reduction in crystallinity of perovskite. The increase in PL intensity induced by $EuBr_2$ doping generally indicates the suppressed the non-radiative recombination caused by trap states. Therefore, we speculate that $EuBr_2$ has chemical passivation effect on defects at grain boundary and surface. However, deducing from the TRPL fitting curve (Fig. 1(e)), one can find that the average carrier lifetime reduces from 173 ns to 155 ns upon $EuBr_2$ doping.[29] As a result, it can be concluded that the trace amount of $EuBr_2$ doping hardly influences the optoelectronic properties of perovskite films and the variation may be originated from the normal fluctuation during measurement.

Furthermore, the effect of $EuBr_2$ doping on photovoltaic performance of PSC was investigated based on a conventional architecture of glass/ITO/SnO_2/perovskite/Spiro-OMeTAD/Au, whose typical *J*–*V* characteristics (Fig. 1(f)) were measured under 1-sun illumination on PSCs with the varying europium contents. As shown in Table 1, a champion PCE of 23.04% is achieved in the device doped with 2.5-μL $EuBr_2$, slightly higher than the control device (22.92%). Further increased europium doping will be detrimental to the device performance. Apparently, the trace amount of europium doping is ineffective in improving the device efficiency.

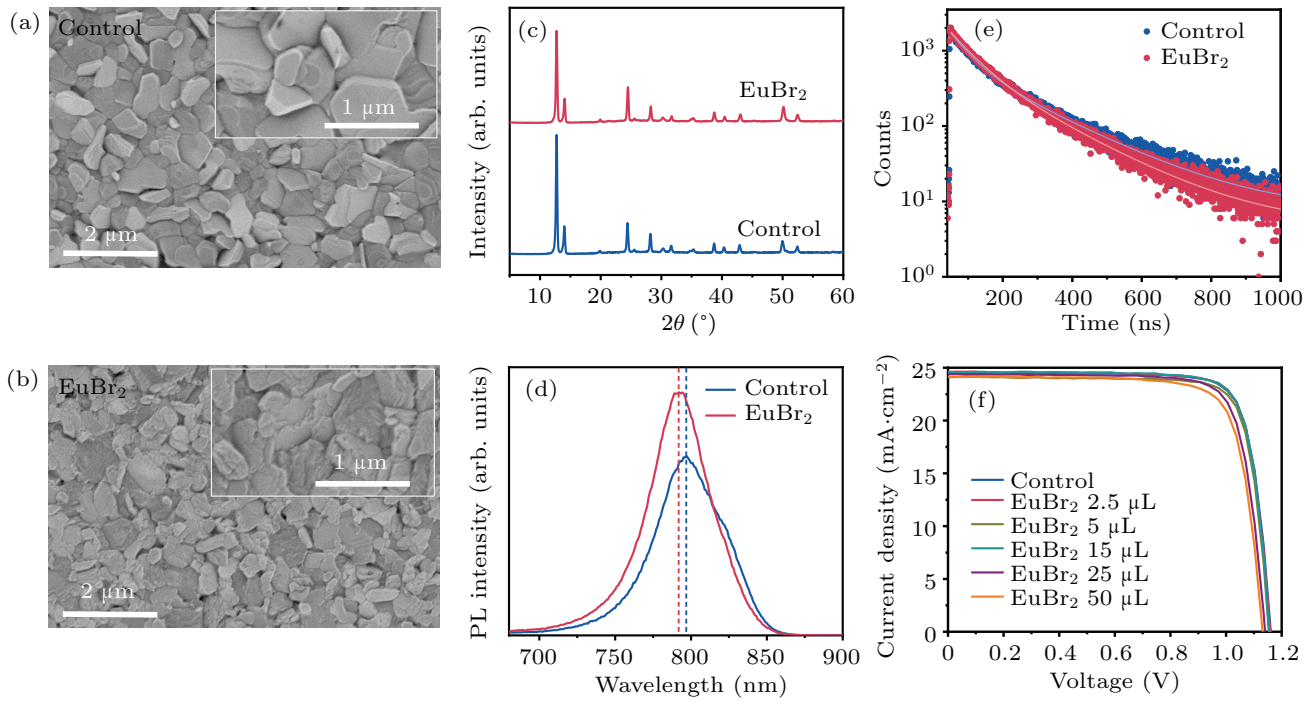


Fig. 1. (a)–(b) SEM images, (c) XRD patterns, (d)–(e) PL and TRPL spectra of control and $EuBr_2$-doped perovskite films, (f) the corresponding reverse scan *J*–*V* curves of PSCs with different $EuBr_2$ doping contents.

Table 1. Detailed PV parameters of devices with different $EuBr_2$ doping contents.

		J_{SC} (mA/cm^2)	V_{OC} (V)	FF	PCE (%)
Control	reverse	24.50	1.15	0.81	22.92
	forward	24.51	1.15	0.80	22.54
2.5 μL	reverse	24.62	1.15	0.81	23.04
	forward	24.64	1.15	0.80	22.59
5 μL	reverse	24.11	1.15	0.81	22.55
	forward	24.10	1.15	0.79	21.91
15 μL	reverse	24.59	1.15	0.81	23.02
	forward	24.60	1.15	0.80	22.68
25 μL	reverse	24.39	1.15	0.79	22.13
	forward	24.38	1.12	0.78	21.21
50 μL	reverse	24.15	1.12	0.79	21.37
	forward	24.13	1.12	0.77	20.77

The stability of the control and $EuBr_2$-doped perovskite films in ambient environment (in air with RH of $\sim$ 40%) was evaluated by XRD measurements, as shown in Figs. 2(a) and 2(b). It is found that, with a storage of 21 days, the control perovskite film becomes yellowish and there is the obvious increase in characteristic diffraction of PbI_2 through comparing to that of the fresh one, indicative of the decomposition of perovskite into PbI_2. Simultaneously, the α phase substantially decreases while δ phase perovskite increases, suggesting that the α–δ phase transition occurs in the control perovskite. Unlike the control film, the $EuBr_2$-doped perovskite film with the same storage days remains black, and the decomposition and degradation become obviously mitigated (Fig. 2(b)). With further increased storage of 43 days, the control film becomes completely yellow and the XRD measurement only shows PbI_2 and δ phases, whereas the black α phase perovskite still exists in the $EuBr_2$-doped film, demonstrating that $EuBr_2$ doping effectively hampers decomposition and the α–δ phase transition. Also, the UV-Vis measurement was conducted to track the degradation processes of both perovskite films. Comparing Figs. 2(c) and 2(d), one sees that the $EuBr_2$ doping remarkably reserves the light absorption of the photovoltaic α phase perovskite. Noticeably, a sharp absorption peak assigned to PbI_2 was observed in the UV-Vis spectra of control films with a storage of either 21 days or 43 days (see Figs. 2(c) and 2(d)), suggestive of the decomposition of perovskite.

Figure 3 shows the XRD patterns and UV-Vis spectra of both control and $EuBr_2$-doped perovskite films under the higher RH condition. Comparing with Fig. 2, it is clear that the high RH makes both control and $EuBr_2$-doped sample degrade faster than the low RH, but the $EuBr_2$-doped sample exhibits a better stability (with the evidently inhibited δ phase) than the control sample. Overall, $EuBr_2$ doping is more effective in mitigating the decomposition and α–δ phase transition in the ambient environment. Further measuring the XRD patterns and the UV-Vis spectra of the perovskite films in air at 85 °C (see Figs. 4(a)–4(c)), we found that both control and $EuBr_2$-doped perovskite films quickly decompose into PbI_2 at 85 °C. It is mainly due to the volatilization of organic component under such a high temperature. Obviously, $EuBr_2$ doping has slight effect on the thermal stability of perovskite film.

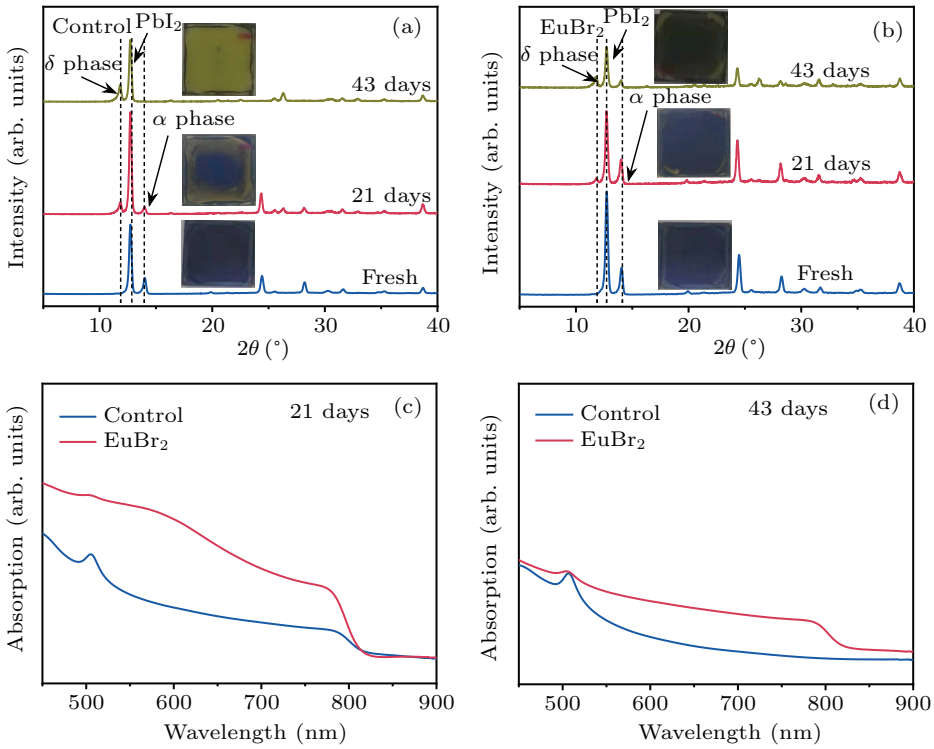


Fig. 2. (a)–(b) Evolution of XRD patterns for control and $EuBr_2$-doped perovskite films stored in air with RH of 20%–40%, the inset pictures are the corresponding images of perovskite films. (c)–(d) UV-Vis spectra of films stored in air with RH of 20%–40% for 21 days and 43 days, respectively.

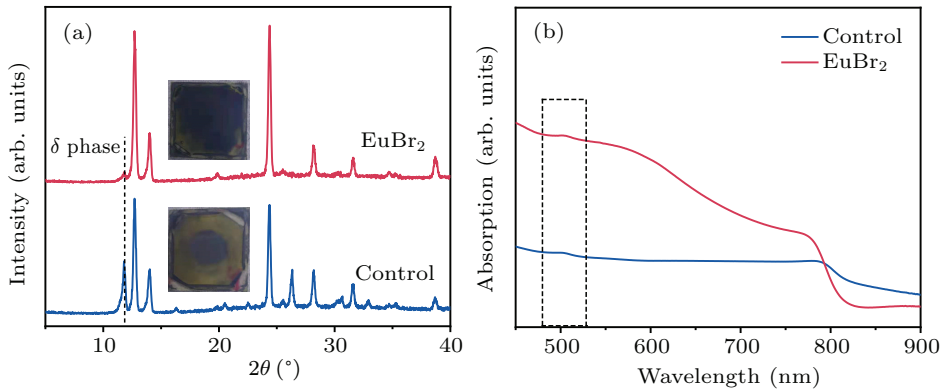


Fig. 3. (a) XRD patterns and (b) UV-Vis spectra evolution of control and $EuBr_2$-doped perovskite films stored in air with RH of 50%–70%, the inset pictures are the corresponding images of perovskite films for 4 days.

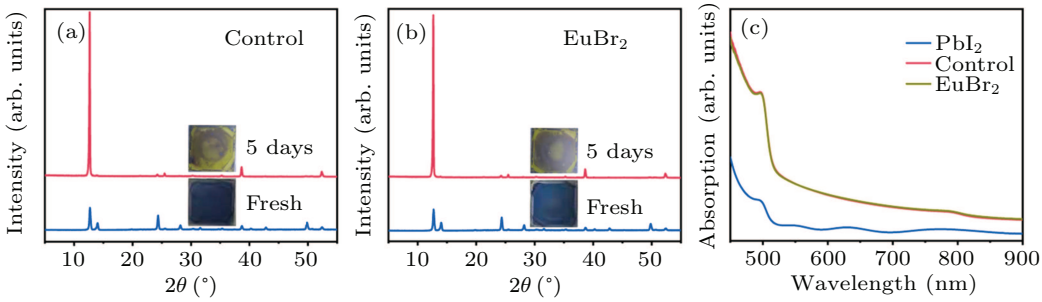


Fig. 4. (a)–(b) XRD patterns and (c) UV-Vis spectra evolution of control and $EuBr_2$-doped perovskite films in air at 85 °C for 5 days, the inset pictures are the corresponding images of perovskite films.

To make clear the mechanism underlying the mitigated decomposition and (α–δ) phase transition induced by $EuBr_2$ doping, we employed the FTIR and XPS measurements to examine the chemical state of $EuBr_2$ in the doped perovskite. It is evident from Fig. 5(a) that there is a unique FTIR absorption peak at 667 cm^{-1} in $EuBr_2$-doped films, which may be attributed to the vibration of chemical bonds related to Eu or Br. The XPS survey spectra of the control and $EuBr_2$-doped

perovskites are shown in Fig. 5(b). Due to the low doping content, Eu and Br were not obvious in the survey spectra, but they were fortunately detected in the high resolution spectra. It is interesting from Fig. 5(c) that Eu^{3+} rather than Eu^{2+} was observed in the doped perovskite, revealing that Eu^{2+} was oxidized during the perovskite fabrication process. The similar phenomenon has been reported by Lei *et al.*, where Eu^{2+} was instantly oxidized into Eu^{3+} in $EuBr_2$-doped $CsBr/PbBr_2$ precursor under ambient environment.[30] In the high resolution spectra of Br 3d (Fig. 5(d)), the peak appears at around 65 eV, which is directly linked to the energy loss of I 4d. It is the mergence of I 4d with the Br 3d (due to the low content of Br element) that hampers the effective analysis of chemical state of Br at this range. Fortunately, the peak at the higher binding energy of 72 eV is detected, which is probably attributed to BrO_3^-. Since it is always difficult to oxidize Br^- into BrO_3^- in N_2 or ambient condition, OH radicals and O_3 are expected to play a crucial role in the oxidization process.[31,32] Considering SnO_2 substrate was treated with UV-ozone before perovskite layer fabrication, it is believed that O_3 and hydroxyl radical absorbed on SnO_2 promote the oxidization of Br^- into BrO_3^-.

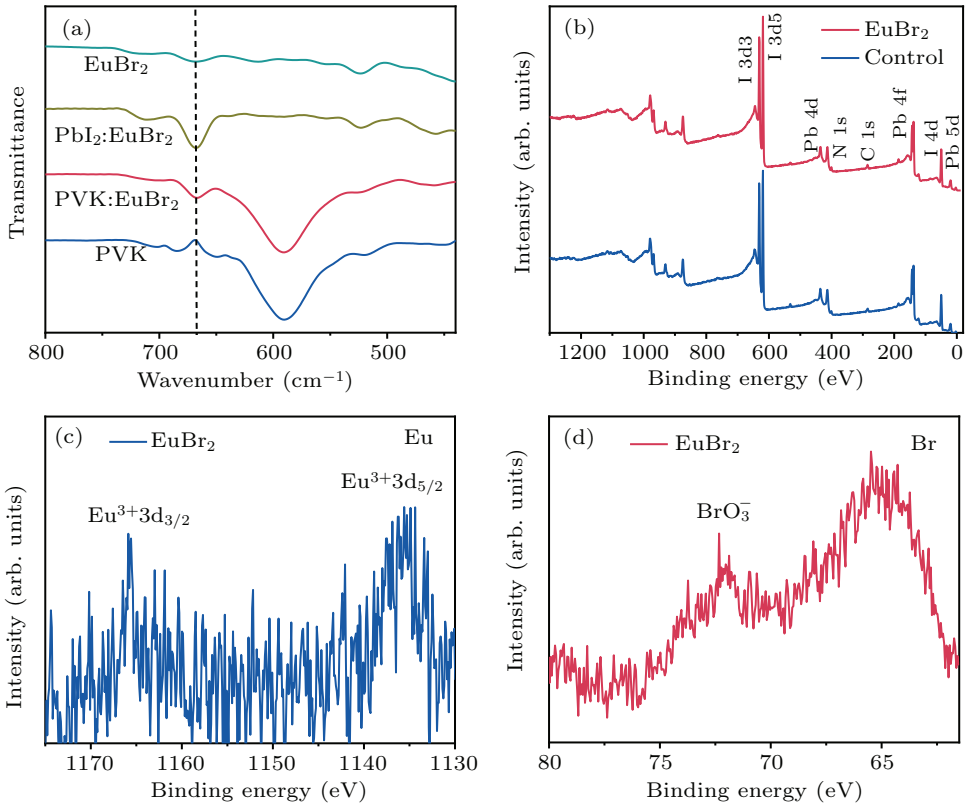


Fig. 5. (a) FTIR spectra of $EuBr_2$, $EuBr_2$:PbI_2, $EuBr_2$-doped perovskite, and control perovskite films measured in air, (b) XPS survey spectra of control and $EuBr_2$-doped perovskite films, (c) high resolution XPS spectra of Eu, (d) high resolution XPS spectra of Br.

Taking the chemical changes of Eu and Br into account, we propose that $EuBr_2$ aggregates at perovskite grain boundaries and surface rather than incorporates directly into perovskite lattice, which partially limits the perovskite grain growth as suggested by SEM and XRD results. Moreover, the oxidization of $EuBr_2$ into $Eu(BrO_3)_3$ is more likely to capture the ambient H_2O by forming $Eu(BrO_3)_3{\cdot}(H_2O)_x$[33,34] to protect perovskite from erosion. H_2O is a key culprit in causing instability in perovskite and devices. As XRD and UV measurements in Fig. 2 suggested, phase transition and decomposition into PbI_2 occurred in perovskite under humidity condition. According to previous report, we suggest initially perovskite absorbs water to form hydrated product. Then, water molecules react with perovskite, leading to phase transition and material decomposition into PbI_2.[35,36] It was reported comparing with Eu^{2+}, the oxidation product Eu^{3+} tends to coordinate with H_2O molecules. Therefore, the oxidization of $EuBr_2$ into $Eu(BrO_3)_3$ hampers H_2O absorbing onto and reacting with perovskite by forming $Eu(BrO_3)_3{\cdot}(H_2O)_x$. Consequently, the resultant phase transition and decomposition is effectively inhibited.

In order to evaluate the thermal stability of the $EuBr_2$-doped PSC, Spiro-OMeTAD was replaced with a more thermal stable PTAA hole transporting material. The corresponding *J*–*V* characteristic curves are shown in Fig. 6(a). The device performance upon europium doping is comparable to the control device. Table 3 shows detailed PV parameters. The champion device with $EuBr_2$ doping delivers an efficiency of

20.7%, slightly higher than the control device (20.1%). Figure 6(b) shows that the efficiency evolution of the control and $EuBr_2$-doped PSCs heated at 85 °C in air with RH of 20%–40% for 13 days. Apparently, without any encapsulation, the harsh operation condition leads to the fast degradation for both devices. But the $EuBr_2$-doped PSC retains 43% of the initial efficiency, much higher than that (22%) of the control device and hence exhibiting the improved stability.

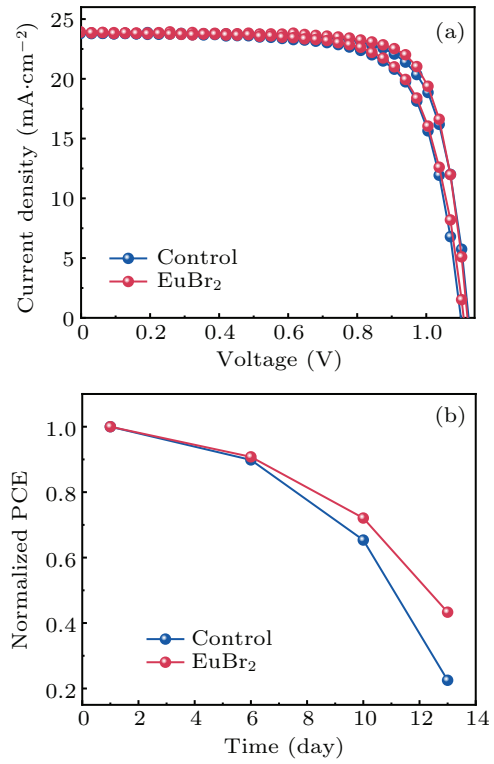


Fig. 6. (a) The *J*–*V* curves of control and $EuBr_2$-doped PSCs with PTAA as HTL, (b) efficiency evolution of control and $EuBr_2$-doped PSCs heated at 85 °C in air with RH of 20%–40% for 13 days.

Table 2. Detailed PV parameters of devices with PTAA as HTL.

		J_{SC} (mA/cm^2)	V_{OC} (V)	FF	PCE (%)
Control	reverse	23.81	1.12	0.76	2.11
	forward	23.81	1.12	0.73	18.88
$EuBr_2$	reverse	23.87	1.12	0.77	2.70
	forward	24.90	1.12	0.71	19.06

4. Conclusion

In summary, we investigated the influence of $EuBr_2$ doping on the perovskite film and device through using the two-step sequential method to dope $EuBr_2$ into perovskite. Results show that $EuBr_2$ doping effectively inhibits the decomposition and α–δ phase transition of perovskite under the ambient environment. Simultaneously, $EuBr_2$ would rather aggregate at grain boundaries and surface of the perovskite film than incorporate into the perovskite lattice, sheltering perovskite from humidity erosion through hampering the penetration of H_2O molecules. $EuBr_2$ doping improves the stability of PSC. Especially, the champion device efficiency of 23.04% is achieved, revealing the effectiveness of $EuBr_2$ doping in promoting the perovskite performance.

Acknowledgements

Project supported by the Fundamental Research Program of Shanxi Province, China (Grant No. 20210302124228), the National Key Research and Development Program of China (Grant No. 2022YFB4200203), the Key Project of Natural Science Foundation of Tianjin (Grant No. 22JCZDJC00120), and the 111 Project (Grant No. B16027).

References

[1] "Best Research-Cell Efficiency Chart, Photovoltaic Research", NREL
[2] Xiong M, Zou W J, Fan K, Qin C C, Li S B, Fei L F, Jiang J Z, Huang H T, Shen L, Gao F, Jen A K Y and Yao K 2022 *ACS Energy Lett.* **7** 550
[3] Azmi R, Ugur E, Seitkhan A, Aljamaan F, Subbiah A S, Liu J, Harrison G T, Nugraha M I, Eswaran M K, Babics M, Chen Y, Xu F Z, Allen T G, Rehman A U, Wang C L, Anthopoulos T D, Schwingenschlög U, Bastiani M D, Aydin E and Wolf S D 2022 *Science* **376** 73
[4] Jang Y W, Lee S, Yeom K M, Jeong K, Choi K, Choi M and Noh J H 2021 *Nat. Energy* **6** 63
[5] Jiang Q, Tong J H, Xian Y M, Kerner R A, Dunfield S P, Xiao C X, Scheidt R A, Kuciauskas D, Wang X, Hautzinger M P, Tirawat R, Beard M C, Fenning D P, Berry J J, Larson B W, Yan Y Y and Zhu K 2022 *Nature* **611** 278
[6] Ma S, Yuan G Z, Zhang Y, Yang N, Li Y J and Chen Q 2022 *Energy Environ. Sci.* **15** 13
[7] Mei A Y, Sheng Y S, Ming Y, Hu Y, Rong Y G, Zhang W H, Luo S L, Na G R, Tian C B, Hou X M, Xiong Y L, Zhang Z H, Liu S, Uchida S, Kim T W, Yuan Y B, Zhang L J, Zhou Y H and Han H W 2020 *Joule* **4** 2646
[8] Zhang S and Han G F 2020 *Prog. Energy* **2** 022002
[9] Eperon G E, Stranks S D, Menelaou C, Johnston M B, Herz L M and Snaith H J 2014 *Energy Environ. Sci.* **7** 982
[10] Han Q F, Bae S H, Sun P Y, Hsieh Y T, Yang Y, Rim Y S, Zhao H X, Chen Q, Shi W Z, Li G and Yang Y 2016 *Adv. Mater.* **28** 2253
[11] Fan Z, Xiao H, Wang Y L, Zhao Z P, Lin Z Y, Cheng H C, Lee S J, Wang G M, Feng Z Y, Goddard W A, Huang Y and Duan X F 2017 *Joule* **1** 548
[12] Abdelmageed G, Mackeen C, Hellier K, Jewell L, Seymour L, Tingwald M, Bridges F, Zhang J Z and Carter S 2018 *Sol. Energy Mater. Sol. Cells* **174** 566
[13] Aristidou N, Sanchez-Molina I, Chotchuangchutchaval T, Brown M, Martinez L, Rath T and Haque S A 2015 *Angew. Chem. Int. Ed.* **54** 8208
[14] Bryant D, Aristidou N, Pont S, Sanchez-Molina I, Chotchunangatchaval T, Wheeler S, Durrant J R and Haque S A 2016 *Energy Environ. Sci.* **9** 1655
[15] Wang Q, Chen B, Liu Y, Deng Y H, Bai Y, Dong Q F and Huang J S 2017 *Energy Environ. Sci.* **10** 516
[16] Yang J, He T W, Li M, Li G X, Liu H R, Xu J J, Zhang M, Zuo W W, Qin R P, Aldamasy M H, Yuan M J, Li Z, Byranvand M M, Saliba M and Abate A 2022 *ACS Energy Lett.* **7** 4451
[17] Zhou T, Xu Z Y, Wang R, Dong X Y, Fu Q and Liu Y S 2022 *Adv. Mater.* **34** 2200705
[18] Bu T L, Li J, Li H Y, Tian C C, Su J, Tong G Q, Ono L K, Wang C, Lin Z P, Chai N Y, Zhang X L, Chang J J, Lu J F, Zhong J, Huang W C, Qi Y B, Cheng Y B and Huang F Z 2021 *Science* **372** 1327
[19] Tomulescu A G, Leonat L N, Neaţu F, Stancu V, Toma V, Derbali S, Neaţu Ş, Rostas A M, Beşleagă C, Pătru R, Pintilie I and Florea M 2021 *Sol. Energy Mater. Sol. Cells* **227** 111096
[20] Chen B B, Wang P Y, Li R J, Ren N Y, Han W, Zhu Z, Wang J, Wang S L, Shi B, Liu J J, Liu P F, Huang Q, Xu S Z, Zhao Y and Zhang X D 2022 *ACS Energy Lett.* **7** 2771
[21] Bai D L, Zhang J R, Jin Z W, Bian H, Wang K, Wang H R, Liang L, Wang Q and Liu S Z 2018 *ACS Energy Lett.* **3** 970

[22] Swarnkar A, Mir W J and Nag A 2018 *ACS Energy Lett.* **3** 286
[23] Syzgantseva O A, Saliba M, Grätzel M and Rothlisberger U 2017 *J. Phys. Chem. Lett.* **8** 1191
[24] Zhao Y, Ma F, Qu Z H, Yu S Q, Shen T, Deng H X, Chu X B, Peng X X, Yuan Y B, Zhang X W and You J B 2022 *Science* **377** 531
[25] Yang S M, Zhao H, Han Y, Duan C Y, Liu Z K and Liu S Z 2019 *Small* **15** 1904387
[26] Karunakaran S K, Arumugam G M, Yang W T, Ge S J, Khan S N, Mai Y H, Lin X Z and Yang G W 2020 *Solar RRL* **4** 2000390
[27] Xiang W C, Wang Z W, Kubicki D J, Tress W, Luo J S, Prochowicz D, Akin S, Emsley L, Zhou J T, Dietler G, Grätzel M and Hagfeldt A 2019 *Joule* **3** 205
[28] Wang L G, Zhou H P, Hu J N, Huang B L, Sun M Z, Dong B W, Zheng G H H, Huang Y, Chen Y H, Li L, Xu Z Q, Li N X, Liu Z, Chen Q, Sun L D and Yan C H 2019 *Science* **363** 265
[29] Hou M N, Xu Y Z, Zhou B, Tian Y, Wu Y, Zhang D K, Wang G C, Li B Z, Ren H Z, Li Y L, Huang Q, Ding Y, Zhao Y, Zhang X D and Hou G F 2020 *Adv. Funct. Mater.* **30** 2002366
[30] Lei J, Chang L Y, Dong Z H and Liu L J 2021 *Mater. Res. Bull.* **137** 111191
[31] Ozekin K, Westerhoff P, Gary L A and Siddiqui M 1998 *J. Environ. Eng.* **124** 456
[32] Van Gunten U 2003 *Water Res.* **37** 1469
[33] Bushiri M J and Nayar V U 2001 *Int. J. Mod. Phys. B* **15** 2499
[34] Tilkens L, Randall K, Sun J, Berry M T, May P S and Yamase T 2004 *J. Phys. Chem. A* **108** 6624
[35] Song Z, Abate A, Watthage S C, Liyanage G K, Phillips A B, Steiner U, Graetzel M and Heben M J 2016 *Adv. Energy Mater.* **6** 1600846
[36] Mosconi E, Azpiroz J M and Angelis F D 2015 *Chem. Mater.* **27** 4885